Integrin-linked kinase tunes cell–cell and cell-matrix adhesions to regulate the switch between apoptosis and EMT downstream of TGFβ1

Ayse Nihan Kilinc[a], Siyang Han[b], Lena A. Barrett[a], Niroshan Anandasivam[a], and Celeste M. Nelson[a,b,*]

[a]Departments of Chemical & Biological Engineering and [b]Molecular Biology, Princeton University, Princeton, NJ 08544

ABSTRACT **Epithelial-mesenchymal transition (EMT) is a morphogenetic process that endows epithelial cells with migratory and invasive potential. Mechanical and chemical signals from the tumor microenvironment can activate the EMT program, thereby permitting cancer cells to invade the surrounding stroma and disseminate to distant organs. Transforming growth factor β1 (TGFβ1) is a potent inducer of EMT that can also induce apoptosis depending on the microenvironmental context. In particular, stiff microenvironments promote EMT while softer ones promote apoptosis. Here, we investigated the molecular signaling downstream of matrix stiffness that regulates the phenotypic switch in response to TGFβ1 and uncovered a critical role for integrin-linked kinase (ILK). Specifically, depleting ILK from mammary epithelial cells precludes their ability to sense the stiffness of their microenvironment. In response to treatment with TGFβ1, ILK-depleted cells undergo apoptosis on both soft and stiff substrata. We found that knockdown of ILK decreases focal adhesions and increases cell–cell adhesions, thus shifting the balance from cell–matrix to cell–cell adhesion. High cell–matrix adhesion promotes EMT whereas high cell–cell adhesion promotes apoptosis downstream of TGFβ1. These results highlight an important role for ILK in controlling cell phenotype by regulating adhesive connections to the local microenvironment.**

Monitoring Editor
Valerie Marie Weaver
University of California, San Francisco

Received: Feb 3, 2020
Revised: Dec 17, 2020
Accepted: Dec 29, 2020

INTRODUCTION

Epithelial-mesenchymal transition (EMT), a morphological and transcriptional program that permits epithelial cells to transdifferentiate into motile mesenchymal cells, occurs during normal embryonic development and tissue regeneration. When activated aberrantly, EMT can contribute pathologically to the metastasis of cancer (Varga and Greten, 2017). During the EMT process, cells down-regulate intercellular adhesions, detach from their neighbors, and up-regulate cell–matrix adhesions to facilitate local invasion and metastatic dissemination (Friedl and Alexander, 2011). This transition is regulated by both mechanical and chemical signals from the surrounding microenvironment. For example, the extracellular matrix (ECM) is stiffer within breast tumors than within the surrounding normal mammary tissue, which correlates with poor survival (Paszek *et al.*, 2005). In response to increased ECM stiffness, the transcription factor Twist1 acts as a mechanomediator to activate EMT (Wei *et al.*, 2015). Moreover, stiff matrices induce the localization of Rac1b to the plasma membrane, thereby promoting the assembly of the NADPH oxidase complex, which activates EMT in response to matrix metalloproteinases (MMPs) (Lee *et al.*, 2012). Stiff matrices have been found to promote EMT in several different epithelial cell types (Lee *et al.*, 2012; Wei *et al.*, 2015; Rice *et al.*, 2017).

Transforming growth factor β1 (TGFβ1) is the most well-studied regulator of EMT within the cellular microenvironment and can also induce apoptosis under some microenvironmental conditions. How cells ultimately decide to undergo EMT or apoptosis in response to TGFβ1 remains unclear, but several studies have suggested context-dependent mechanisms. Mouse mammary epithelial cells were found to become resistant to TGFβ1-induced apoptosis after chronic exposure to the ligand, which suppresses pro-apoptotic pathways

This article was published online ahead of print in MBoC in Press (http://www.molbiolcell.org/cgi/doi/10.1091/mbc.E20-02-0092) on January 6, 2021.

Competing interests: The authors declare no competing or financial interest.

*Address correspondence to: Celeste M. Nelson (celesten@princeton.edu).

Abbreviations used: ECM, extracellular matrix; EMT, epithelial-mesenchymal transition; ILK, integrin-linked kinase; MMP, matrix metalloproteinase; PBS, phosphate-buffered saline; PDMS, polydimethylsiloxane; shRNA, short hairpin RNA; TGF, transforming growth factor.

(Gal *et al.*, 2008). In mouse liver epithelial cells, TGFβ1 induces apoptosis or EMT depending on the stage of the cell cycle, with apoptosis and EMT taking place during G2/M and G1/S, respectively (Yang *et al.*, 2006). In human retinal pigment epithelial cells, TGFβ1 was shown to regulate the cell cycle through survivin and, thus, the switch between EMT and apoptosis (Lee *et al.*, 2013). ECM stiffness also regulates cell fate downstream of TGFβ1 in both canine kidney and mouse mammary epithelial cells—soft matrices promote apoptosis, whereas stiff matrices promote EMT (Leight *et al.*, 2012).

Mechanical signals from the cellular microenvironment are translated into biochemical signaling cascades through cellular mechanotransduction, which enables cells to sense, respond, and adapt to their physical surroundings. This process is largely mediated by integrin signaling. Integrins bind to specific motifs in ECM proteins such as fibronectin, whereas their cytoplasmic tails associate with linker proteins including talin, vinculin, and integrin-linked kinase (ILK). ILK, interacting with parvin (which binds to paxillin and actin) and PINCH, takes part in transmitting forces from integrins to the actin cytoskeleton and in forming functional focal adhesion complexes (Elad *et al.*, 2013). ILK plays a fundamental role in many different signaling pathways and cell behaviors including EMT. Overexpression of ILK causes human kidney and mouse mammary epithelial cells to acquire a mesenchymal morphology, in part by disrupting cell–cell adhesions (Somasiri *et al.*, 2001; Li *et al.*, 2003). Conversely, we recently found that depleting ILK abolishes the ability of cells to change their morphology in response to ECM stiffness—mammary epithelial cells that normally spread out on stiff substrata exhibit a rounded morphology when ILK is down-regulated (Han *et al.*, 2018).

Here, we examined the mechanism by which matrix stiffness controls the fate of mammary epithelial cells in response to treatment with TGFβ1. Specifically, we focused on signaling from the ECM through ILK. We used engineered synthetic substrata to mimic the mechanical stiffnesses of the normal mammary gland and of breast tumors. We found that ILK modulates how NMuMG mouse mammary epithelial cells respond to TGFβ1 in a stiffness-dependent and time-dependent manner: knockdown of ILK prevents EMT in the first 24 h of exposure to TGFβ1 in mammary epithelial cells cultured on both soft and stiff substrata; after 48 h of treatment with TGFβ1, a small population of ILK-depleted mammary epithelial cells undergo EMT only on stiff substrata while the majority of these cells undergo apoptosis. Moreover, depletion of ILK and culture on soft microenvironments synergistically promote TGFβ1-induced apoptosis. We further found that depletion of ILK increases the membrane localization of cell–cell adhesion proteins and decreases the activation of focal adhesion proteins, suggesting that ILK regulates the balance between cell–cell and cell–ECM adhesion. Through balancing adhesion to the microenvironment, ILK controls the functional switch between EMT and apoptosis downstream of TGFβ1. Taken together, our results suggest a central role for ILK in tuning the relative strength of cell–cell and cell–matrix adhesions, which represents critical input in cell-fate decisions downstream of TGFβ1.

RESULTS

Soft substrata and loss of ILK promote apoptosis in response to TGFβ1

We previously found that stably depleting ILK using short hairpin RNA (shRNA) leads to a striking change in the morphology of NMuMG mouse mammary epithelial cells (Figure 1, A and B) (Han *et al.*, 2018). Specifically, control NMuMG cells (shcntl) exhibit an elongated, well-spread, and spindle-like morphology when cultured on stiff substratum with an elastic modulus similar to that of mammary tumors (*E*~4020 Pa). When cultured on a soft substratum that has a stiffness similar to that of the normal mammary gland (*E*~130 Pa), shcntl cells are rounded and form multicellular clusters that resemble the structure of mammary acini. Although depleting ILK (shILK) does not alter cell morphology on soft substrata, this manipulation causes cells to exhibit a rounded morphology on stiff substrata. These morphologies strongly resemble the epithelial-like morphology before EMT and the mesenchymal-like morphology after, which inspired us to examine the role of ILK in EMT.

To understand how ILK expression affects the EMT process, we performed time-lapse imaging analysis of shcntl and shILK cells cultured on soft or stiff substrata in the presence or absence of TGFβ1. We found that on soft substrata, cells start to detach from the matrix within 24 h of exposure to TGFβ1, irrespective of ILK levels (Figure 1C). Most cells have completely detached from soft substrata within 48 h of exposure to TGFβ1 (Figure 1C). However, on stiff substrata, treatment with TGFβ1 only induces detachment of shILK cells. In contrast, shcntl cells cultured on stiff substrata adopt an elongated and spindle-like morphology within 24 h of TGFβ1 exposure, consistent with an EMT phenotype. Surprisingly, we observed a similar spindle-like morphology in the few shILK cells that remain anchored on stiff substrata after 48 h of exposure to TGFβ1 (Figure 1C). To determine whether the detachment of shILK cells is the result of apoptosis at earlier time points, we used a fluorometric assay to examine the activity of caspase-3 after 24 h of TGFβ treatment. As expected, this analysis confirmed that depletion of ILK in cells on both soft and stiff microenvironments synergistically promotes apoptosis, instead of EMT, downstream of TGFβ1 (Figure 1D).

ILK depletion prevents TGFβ1-induced EMT in mammary epithelial cells in a time- and stiffness-dependent manner

Because its depletion results in the detachment of cells and a delayed EMT morphology in the cells that remain anchored after prolonged TGFβ1 treatment, we speculated that ILK may regulate the switch between EMT and apoptosis. To test this hypothesis, we cultured shcntl and shILK cells on soft or stiff substrata in the presence or absence of TGFβ1 for 24 h and assayed for the expression of several EMT markers using immunoblotting and immunofluorescence analysis. Depletion of ILK itself promotes an increase in the expression of the epithelial marker E-cadherin and decreases in that of the mesenchymal markers αSMA, Snail, and vimentin in cells on stiff substrata (Figure 2, A and B). Treatment of shcntl cells with TGFβ1 for 24 h induces changes in expression consistent with an EMT program, including down-regulation of E-cadherin (Figure 2, A–C) and ZO1 (Supplemental Figure S1) and up-regulation of αSMA, Snail, and vimentin (Figure 2, A–C) on stiff substrata, as well as in the few cells that remain attached on soft substrata. In contrast, depletion of ILK abolishes the induction of EMT by TGFβ1; cell–cell contacts remain intact and the expression levels of E-cadherin, αSMA, and Snail remain relatively unchanged. Consistently, shILK cells are less migratory than controls (Supplemental Figure S2). These data show that the expression of ILK is required for TGFβ1 to induce EMT in NMuMG mouse mammary epithelial cells.

After 48 h of exposure to TGFβ1, shcntl cells continue to show decreased expression of E-cadherin and ZO1 and increased expression of Snail and αSMA (Figure 3, A and B) on both soft and stiff substrata, as expected. The few shILK cells that remain attached on stiff substrata show a decrease in E-cadherin localization to cell–cell contacts and increased levels of Snail and αSMA (Figure 3). The low numbers of shcntl cells that remain anchored on soft substrata and the similarly low numbers of shILK cells that remain on both microenvironments precluded us from performing immunoblotting analysis at this late time point.

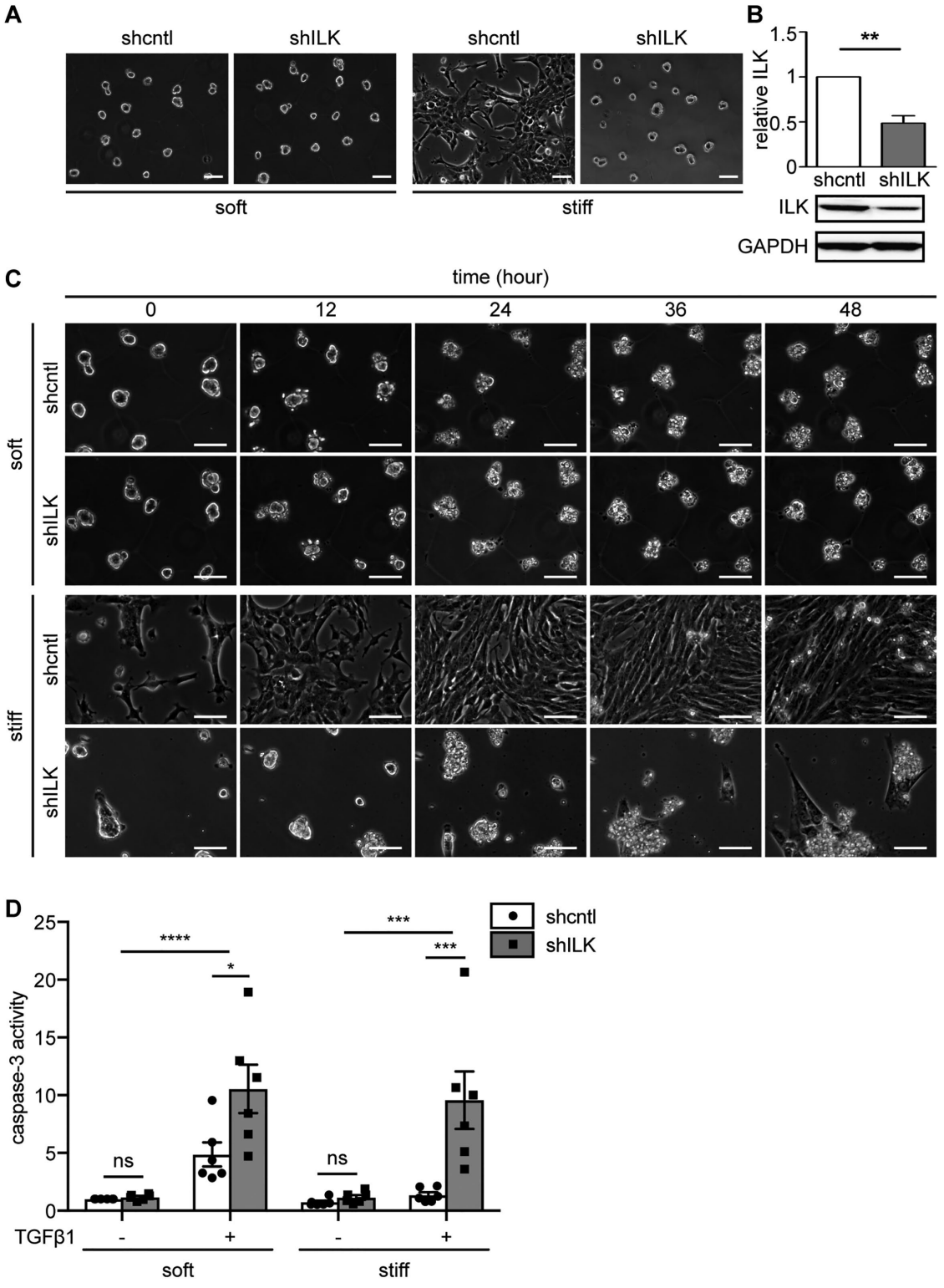

FIGURE 1: Depletion of ILK and culture on soft substrata synergistically promote TGFβ1-induced apoptosis in NMuMG mouse mammary epithelial cells. (A) Phase-contrast images of shcntl and shILK cells cultured on soft (*E*~130 Pa) or stiff (*E*~4020 Pa) fibronectin-coated polyacrylamide substrata. Scale bars, 50 μm. (B) Immunoblotting analysis for ILK normalized to GAPDH in lysates from shcntl and shILK cells. (C) Phase-contrast images of shcntl and shILK cells cultured on soft or stiff substrata and treated with TGFβ1 (2 ng/ml). Scale bars, 100 μm. (D) Quantification of caspase-3 activity in shcntl and shILK cells cultured on soft or stiff substrata and treated with or without TGFβ1 for 24 h. Error bars represent SEM of three (B) or six (D) independent replicates; ns, not significant; $*P < 0.05$; $**P < 0.01$; $***P < 0.001$; $****P < 0.0001$.

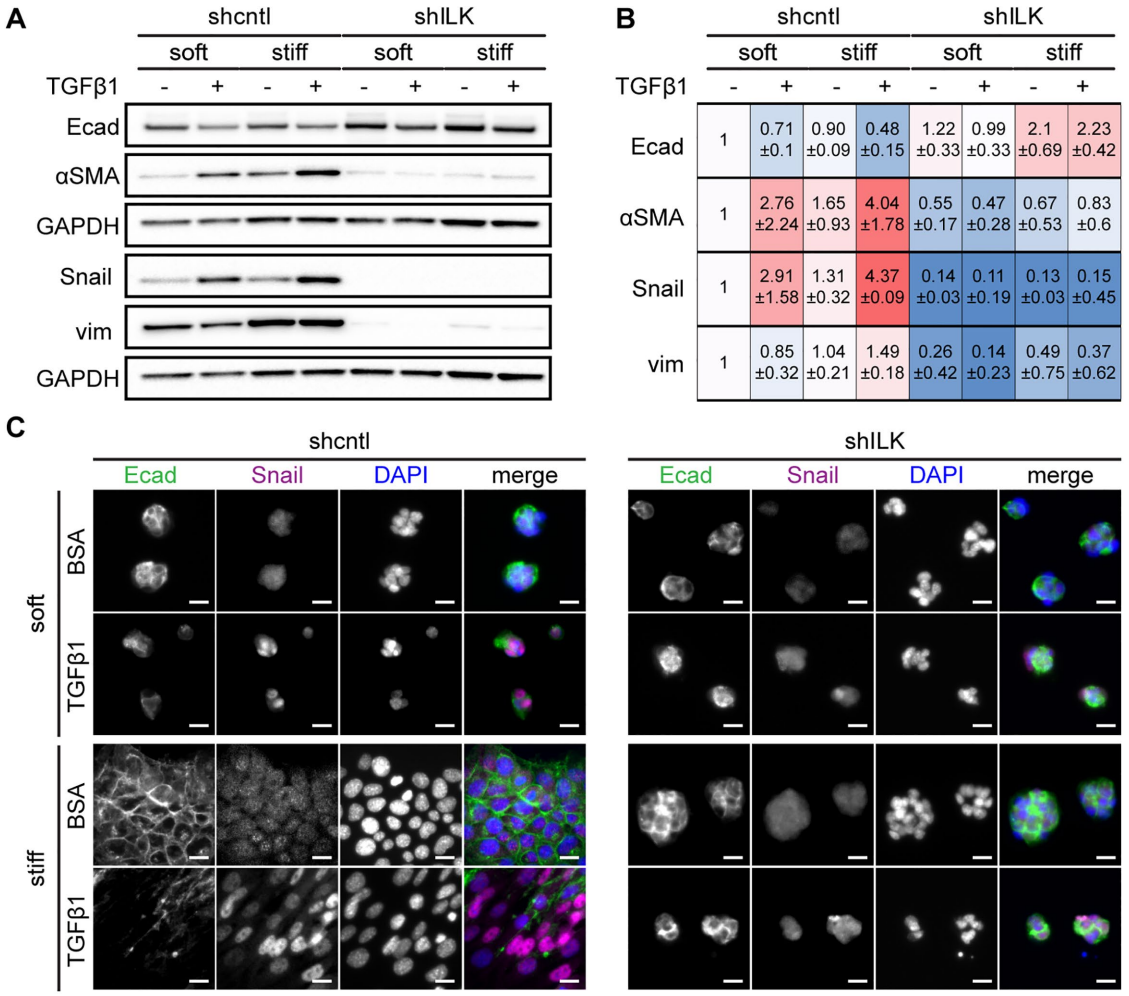

FIGURE 2: Depletion of ILK prevents TGFβ1-induced EMT in NMuMG mouse mammary epithelial cells. (A) Immunoblotting analysis for E-cadherin, αSMA, Snail, vimentin, or GAPDH in shcntl and shILK cells cultured on soft or stiff substrata and treated with or without TGFβ1 for 24 h; immunoblotting replicates are shown in Supplemental Figure S1. (B) Quantification of immunoblotting analysis; shown are mean ± SD of three independent replicates. Color coding indicates relative increase (red) or decrease (blue) in expression, compared with shcntl cells on soft substrata in the absence of TGFβ1. (C) Immunofluorescence analysis for E-cadherin (green), Snail (magenta), and nuclei (blue) in shcntl and shILK cells cultured on soft or stiff substrata and treated with or without TGFβ1 for 24 h. Scale bars, 10 μm.

Depletion of ILK decreases the activation of focal adhesion proteins

Our data suggest that the switch between EMT and apoptosis downstream of TGFβ1 may be associated with ILK-mediated changes in adhesion and mechanosensing. The likelihood of this possibility was strengthened by following the shapes of cells retrospectively in response to treatment with TGFβ1. We carried out time-lapse imaging analysis, identified cells that underwent EMT or apoptosis, and then followed those cells retrospectively in time. We found that cells that eventually underwent apoptosis maintained a rounded morphology, while those that eventually underwent EMT exhibited a more irregular shape, generating protrusions throughout the 48 h of TGFβ1 treatment (Supplemental Figure S3). These data indicate that cells that maintain cell–ECM adhesions are able to undergo EMT in response to TGFβ1.

To determine the effects of ILK on cell–matrix adhesion, we examined the expression and localization of focal adhesion proteins by immunoblotting and immunofluorescence analysis. We found that depletion of ILK does not affect the total levels of FAK (Figure 4A) or paxillin (Figure 4B), but significantly decreases the levels of activated FAK (pY397-FAK) and activated paxillin (pY118-paxillin) (Figure 4, A and B; Supplemental Figure S4). Immunoblotting analysis also revealed that FAK and paxillin are phosphorylated and activated in control cells on stiff substratum and that this regulation is abolished in shILK cells (Figure 4, A and B; Supplemental Figure S4). The levels of total FAK and total paxillin are not affected by substratum stiffness (Figure 4, A and B). Consistently, immunofluorescence analysis of cells cultured on plastic revealed that depletion of ILK causes an enrichment of cortical actin and decreases the formation of cell–matrix adhesions containing activated FAK and paxillin (Figure 4, C–F). Depleting ILK thus reduces cell–matrix adhesion in mammary epithelial cells.

Depletion of ILK increases cell–cell adhesion

Cortical actin is often associated with cadherin-based cell–cell adhesions (Ratheesh and Yap, 2012; Bachir *et al.*, 2017). That we found an increase in cortical actin in shILK cells suggested that ILK expression may regulate adherens junctions. Indeed, immunofluorescence analysis revealed elevated levels of α-catenin, β-catenin, and cortical actin at sites of intercellular contact in shILK cells cultured on

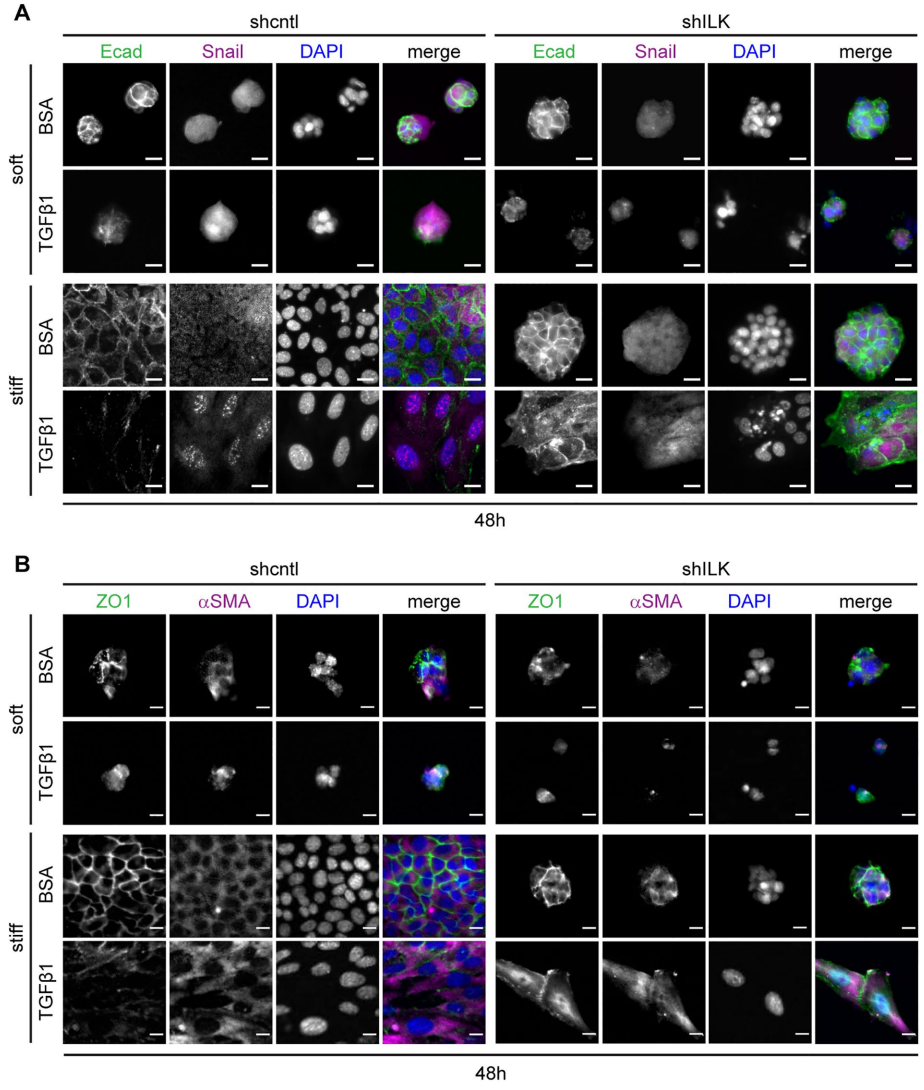

FIGURE 3: On stiff substrata, depletion of ILK leads to either cell detachment or a delayed EMT after prolonged exposure to TGFβ1. Immunofluorescence analysis for (A) E-cadherin (green), Snail (magenta), and nuclei (blue), or (B) ZO1 (green), αSMA (magenta), and nuclei (blue) in shcntl and shILK cells cultured on soft or stiff substrata and treated with or without TGFβ1 for 48 h. Scale bars, 10 μm.

plastic compared with controls (Figure 5, A and B). Consistent with our findings on stiff substrata (Figure 2A), immunoblotting analysis revealed an increase in the levels of E-cadherin and α-catenin in shILK cells cultured on plastic as compared with controls (Figure 5C). The association of adherens junction proteins with the actin cytoskeleton correlates with strong cell–cell interactions (Mege and Ishiyama, 2017). To quantify the extent to which adherens junction components are associated with the cytoskeleton in shILK cells, we measured the distribution of E-cadherin, α-catenin, and β-catenin in Triton X–100-fractionated cell lysates. We found a robust increase in the level of cytoskeleton-associated β-catenin, as indicated by the Triton X-100-insoluble fraction, in shILK cells as compared with controls (Figure 5D). However, the total level of β-catenin is relatively unchanged in response to depletion of ILK (Figure 5C). Therefore, depleting ILK expression enhances adherens junctions in NMuMG cells. These data reveal that the decrease in cell–matrix adhesion associated with loss of ILK is balanced or compensated by an increase in cell–cell adhesion.

The balance between cell–ECM and cell–cell adhesion regulates the switch between EMT and apoptosis downstream of TGFβ1

Since shILK cells show enhanced cell–cell adhesion and preferentially undergo apoptosis instead of EMT in response to TGFβ1, we hypothesized that experimentally decreasing cell–cell adhesion may permit TGFβ1 to induce EMT in these cells. Previous studies have reported that disrupting cell–cell adhesion using function-blocking anti-E-cadherin antibodies or shRNA-mediated knockdown promotes the expression of mesenchymal markers and the acquisition of a mesenchymal morphology in mammary and kidney epithelial cells (Behrens *et al.*, 1989; Qin *et al.*, 2005; Lehembre *et al.*, 2008). Conversely, manipulating cell–cell adhesion by plating cells at different densities also affects the expression of epithelial and mesenchymal markers in mammary epithelial cells, with decreased E-cadherin and increased vimentin at low densities (Cichon *et al.*, 2015). We therefore needed an alternative approach to test our hypothesis. We cultured shcntl and shILK cells on substrata micropatterned with single-cell-sized islands to promote the isolation of individual cells from their neighbors and thus achieve low cell–cell adhesion in both cell types at the same density. We used islands sufficiently large (900 μm^2) to permit cells to spread to the same extent as those on stiff substrata in the presence of TGFβ1 (650 μm^2), but small enough that we were able to capture individual cells on a fraction of the islands. Curiously, we observed that a fraction of the isolated cells express the mesenchymal marker vimentin, even before exposure to TGFβ1, regardless of ILK levels. Nonetheless, we found that treating both micropatterned shcntl and shILK cells with TGFβ1 for 24 h increases the fraction of cells that express vimentin, consistent with the promotion of an EMT phenotype (Figure 6, A and B). In contrast, we found low levels of apoptosis in single micropatterned cells, as inferred from staining for cleaved caspase-3 (Figure 6, C and D). Instead, we found that TGFβ1 induces high levels of apoptosis in cells located within multicellular clusters on the micropatterned islands (Figure 6, C and D). Our results suggest that low cell–cell adhesion promotes EMT in response to TGFβ1, rather than apoptosis, irrespective of ILK expression.

Conversely, to determine whether low cell–ECM adhesion promotes apoptosis in response to TGFβ1, we pharmacologically inhibited FAK in NMuMG cells cultured on soft or stiff substrata in the presence or absence of TGFβ1. We treated cells with increasing concentrations of the FAK inhibitor PF-573228 and 'as expected' found that the levels of pY397-FAK decrease as inhibitor concentration increases (Figure 7A). Caspase-3 activity analysis revealed significantly higher levels of apoptosis in FAK-inhibited cells that were treated with TGFβ1 than in vehicle-treated controls (Figure 7B). Therefore, low cell–cell and high cell–ECM adhesion favors EMT,

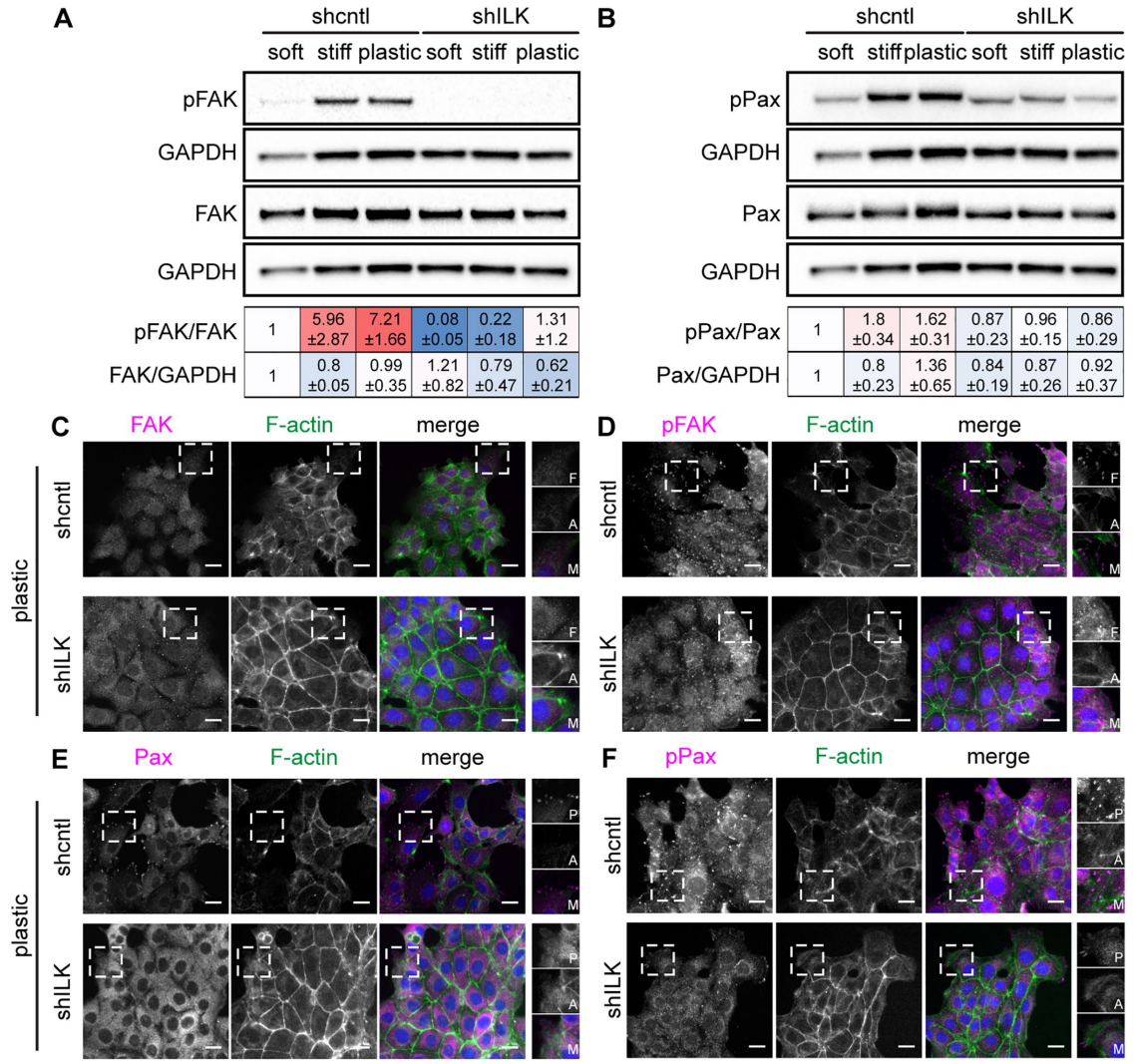

FIGURE 4: Depletion of ILK decreases the activation and assembly of focal adhesion proteins. Immunoblotting analysis for GAPDH and (A) total FAK, pY397-FAK (pFAK), (B) total paxillin (Pax), and pY118-paxillin (pPax) in shcntl and shILK cells cultured on soft or stiff substrata. Quantification shows mean ± SD for three independent experiments; immunoblotting replicates and statistical analysis are shown in Supplemental Figure S4. Immunofluorescence analysis for F-actin (green), nuclei (blue), and (C) FAK (magenta), (D) pFAK (magenta), (E) Pax (magenta), or (F) pPax (magenta) in shcntl and shILK cells cultured on plastic. Scale bars, 20 μm.

whereas high cell–cell and low cell–ECM adhesion favors apoptosis in response to TGFβ1. Surprisingly, previous work found that reducing FAK activity, which would be expected to decrease mechanosensing, is not sufficient to alter apoptosis on stiff substrata (Leight *et al.*, 2012); however, that study used lower concentrations of the FAK inhibitor, which may explain their observation. Our data show that the mechanical stiffness of the microenvironment signals through ILK to tune the relative balance of cell–cell to cell–matrix adhesion, which in turn defines the phenotypic response to TGFβ1.

DISCUSSION

Here we demonstrate that ILK controls the fate of mammary epithelial cells downstream of TGFβ1 by modulating the balance between cell–cell and cell–matrix adhesion. Specifically, depletion of ILK leads to increased cortical actin and adherens junctions and decreased focal adhesions. This promotes apoptosis and suppresses/delays EMT in response to TGFβ1, regardless of matrix stiffness. These results are consistent with a previous study, which found that overexpression of ILK causes mammary epithelial cells to lose the adherens junction protein E-cadherin and reorganize cortical actin into stress fibers (Somasiri *et al.*, 2001). Similarly, soft matrices promote apoptosis downstream of TGFβ1 while stiff matrices promote EMT, consistent with previous findings (Leight *et al.*, 2012), suggesting that depletion of ILK disrupts the ability of cells to sense the mechanical stiffness of their microenvironment. This is not surprising given the essential role for ILK in integrin signaling and focal adhesion assembly. However, when ILK-deficient mammary epithelial cells are cultured as individual cells on micropatterned islands and thus prevented from forming cell–cell adhesions, exposure to TGFβ1 increases the fraction of cells that express the mesenchymal marker vimentin. Our results highlight the role of ILK in regulating the cooperation between cell–cell and cell–matrix adhesions in response to the stiffness of the microenvironment, which governs cell-fate decisions downstream of TGFβ1 (Figure 8).

Stiff microenvironments were previously found to promote EMT. Increased ECM stiffness regulates the PI3K/Akt signaling pathway to activate EMT downstream of TGFβ1 in mammary epithelial cells (Leight *et al.*, 2012). In addition, increased matrix stiffness induces

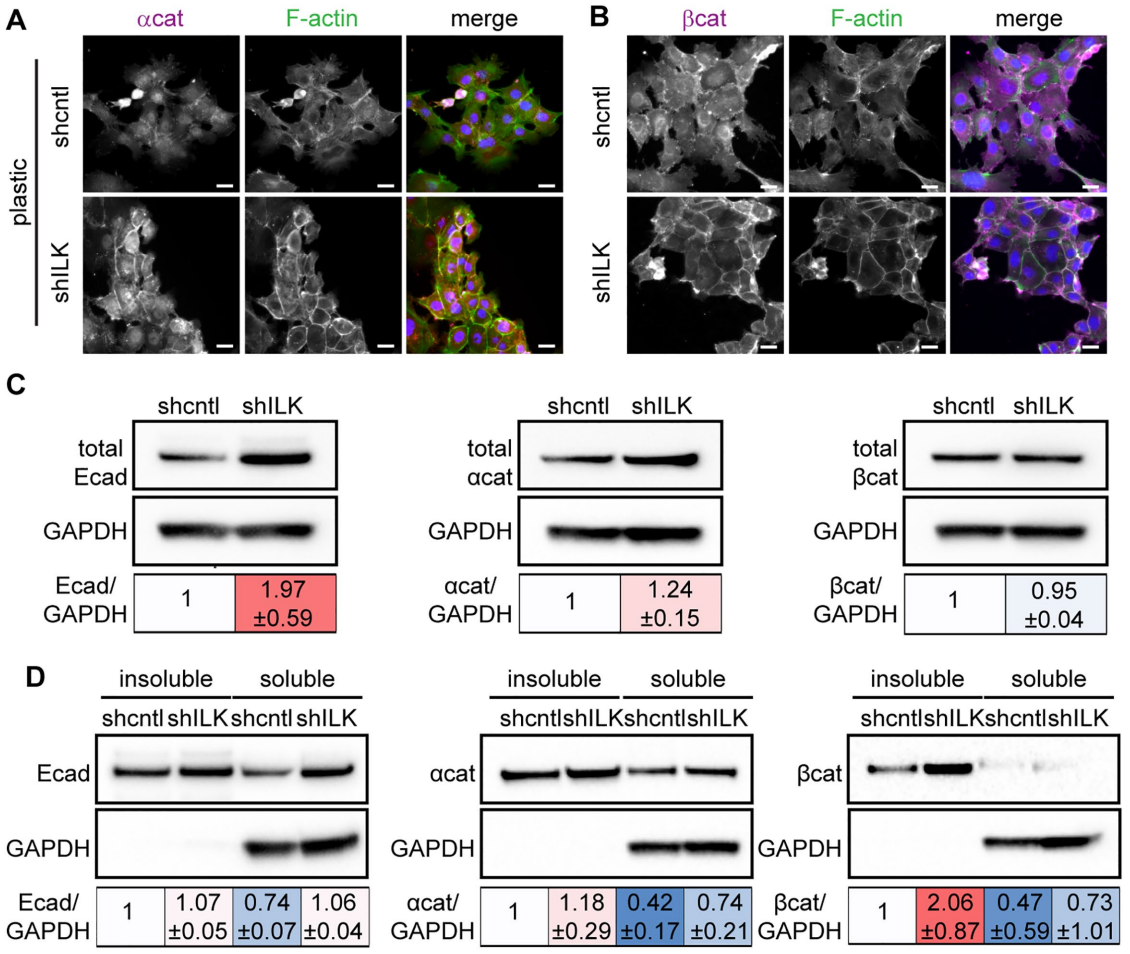

FIGURE 5: Depletion of ILK strengthens cell–cell adhesion. Immunofluorescence analysis for F-actin (green), nuclei (blue), and (A) α-catenin (αcat; magenta) or (B) β-catenin (βcat; magenta) in shcntl and shILK cells. Scale bars, 20 μm. (C) Immunoblotting analysis for E-cadherin (Ecad), αcat, and βcat in shcntl and shILK cells. (D) Immunoblotting analysis for Triton X-100-insoluble or soluble fractions of Ecad, αcat, and βcat in lysates from shcntl and shILK cells. Quantification shows mean ± SD for three independent experiments; immunoblotting replicates and statistical analysis are shown in Supplemental Figure S5.

the nuclear translocation of Twist1, an EMT-associated transcription factor, by releasing it from its cytoplasmic binding partner G3BP2 (Wei *et al.*, 2015). In a mouse model of pancreatic cancer, fibrotic stiffening increases vimentin expression, decreases E-cadherin expression, and induces a mesenchymal morphology, consistent with an EMT program (Rice *et al.*, 2017). Our data add to the underlying mechanism of this regulation. Even in the absence of TGFβ1, depletion of ILK reduces the expression of Snail, suggesting that ILK (and cell–ECM adhesion) positively regulates Snail. Snail has been shown to confer resistance to apoptosis downstream of TGFβ1 and is sufficient to trigger EMT (Franco *et al.*, 2010). Given that stiff microenvironments up-regulate the expression of ILK (Han *et al.*, 2018), it is possible that stiff matrices prime cells to undergo EMT through ILK-mediated signaling through Snail. Moreover, we found that depleting ILK prevents EMT on stiff substrata after 24 h of treatment with TGFβ1, consistent with previous work (Serrano *et al.*, 2013). Of interest, after 48 h of exposure to TGFβ1, the majority of cells that lack ILK have detached and the remaining cells have undergone EMT. Based on our analysis of focal adhesions and our single-cell micropatterning experiments, we speculate that the few shILK cells that remain anchored might have relatively stronger focal adhesions (but still weaker than those in control cells), and are thus rescued from apoptosis and able to undergo EMT after prolonged exposure to TGFβ1. In line with this, signaling through FAK is required for transcriptional up-regulation of mesechymal markers and delocalization of membrane-associated E-cadherin downstream of TGFβ1 in murine hepatocytes (Cicchini *et al.*, 2008). These results suggest that the promotion of EMT by substratum stiffness is not a binary decision—the rate at which the transition takes place may depend on the relative extent of focal adhesion engagement.

Apoptosis and EMT are two fundamental cellular behaviors that are tightly controlled by TGFβ1. In the context of cancer, TGFβ1 can suppress tumor progression by inducing cell death (Guasch *et al.*, 2007) or promote cancer cell invasion and dissemination by stimulating EMT (Heldin *et al.*, 2012). The diverse downstream consequences of exposure to TGFβ1 raise several questions: why does TGFβ1 stimulate apoptosis in some cells and EMT in others? Is there a default cellular fate downstream of TGFβ1 and, if so, under what circumstances will the other fate be activated? Some studies have suggested that cell-fate decisions downstream of TGFβ1 are cell cycle-dependent (Yang *et al.*, 2006; Iordanskaia and Nawshad, 2011; Lee *et al.*, 2013). Our results suggest an alternative but not mutually exclusive mechanism, in which high cell–matrix adhesion promotes EMT whereas high cell–cell adhesion promotes apoptosis.

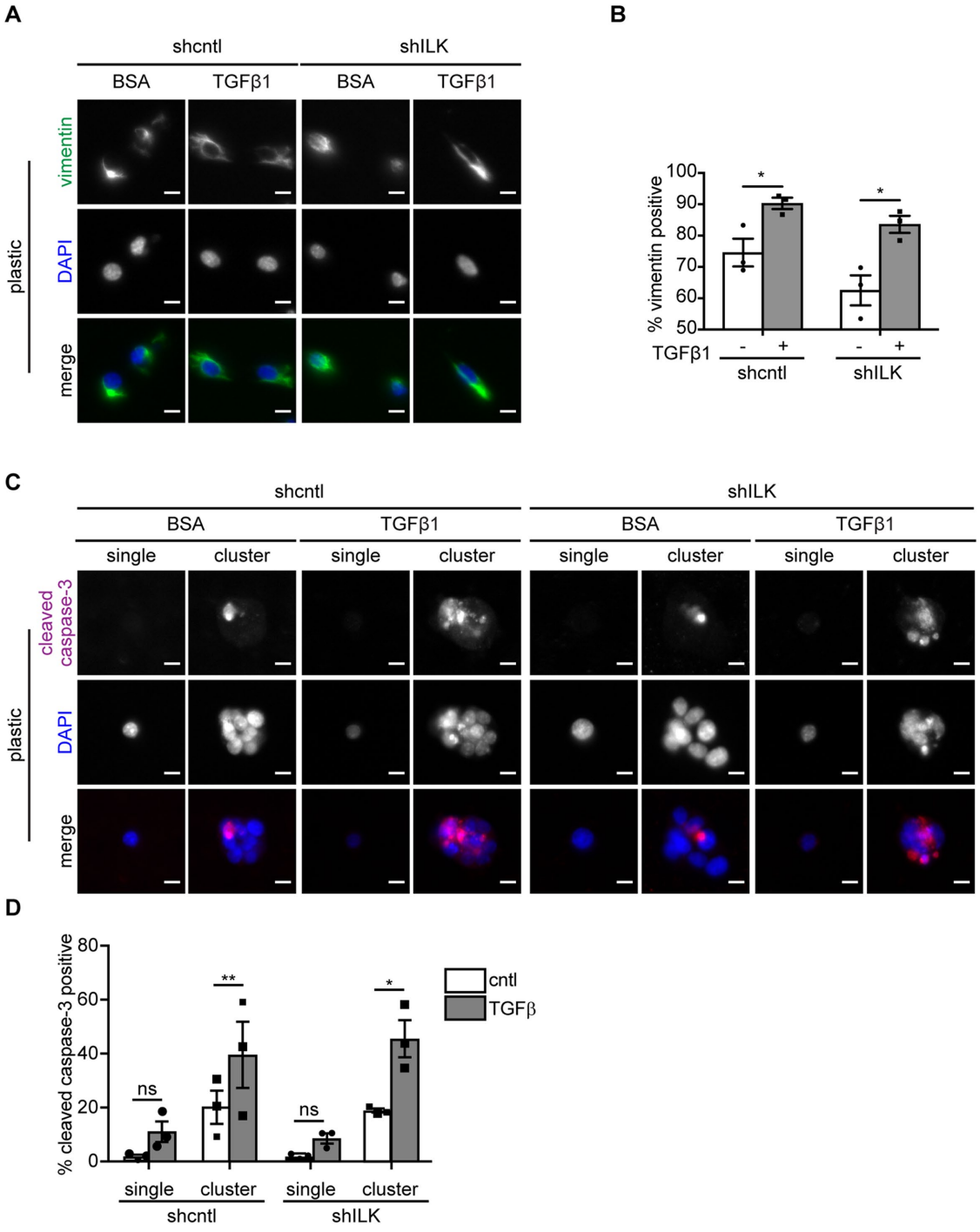

FIGURE 6: Low cell–cell adhesion promotes TGFβ1-induced EMT. (A) Immunofluorescence analysis for vimentin (green) and nuclei (blue) in shcntl and shILK cells on micropatterns treated with or without TGFβ1 for 24 h. Scale bars, 10 μm. (B) Quantification of the percentage of vimentin-positive single shcntl and shILK cells cultured on micropatterned substrata treated with or without TGFβ1 for 24 h. (C) Immunofluorescence analysis for cleaved caspase-3 (magenta) and nuclei (blue) in shcntl and shILK cells on micropatterns treated with or without TGFβ1 for 24 h. Scale bars, 10 μm. (D) Quantification of the percentage of cleaved caspase-3-positive shcntl and shILK cells cultured individually or as clusters on micropatterned substrata and treated with or without TGFβ1 for 24 h. Error bars represent SEM of three independent replicates; each replicate contains at least 200 cells per condition. *$P < 0.05$; **$P < 0.01$.

Cadherin-based adherens junctions and integrin-based focal adhesions are intrinsically linked by the actin cytoskeleton. In response to mechanical stimuli, these two classes of adhesions engage common signaling proteins to remodel the actin cytoskeleton and coordinate intracellular and intercellular force transmission, forming an adhesive network that regulates several cellular functions (Weber *et al.*, 2011; Mui *et al.*, 2016). Engagement of one type of adhesion may alter the other type of adhesion. This cross-talk facilitates morphogenesis in embryonic development and enables tensional homeostasis in healthy tissue. However, this interdependence may

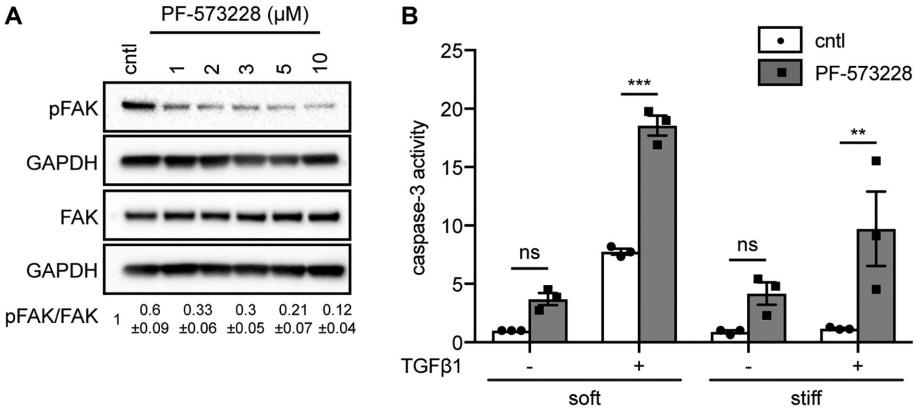

FIGURE 7: Low cell–matrix adhesion promotes TGFβ1-induced apoptosis. (A) Immunoblotting analysis for pFAK, total FAK, and GAPDH in cells treated with different concentrations of the FAK inhibitor PF-573228. Quantification shows mean ± SD for three independent experiments; immunoblotting replicates are shown in Supplemental Figure S6. (B) Quantification of caspase-3 activity in cells cultured on soft or stiff substrata in the presence or absence of PF-573228 (5 μM) and treated with or without TGFβ1 for 24 h. Error bars represent SEM of three independent replicates. $^{**}P < 0.01$; $^{***}P < 0.001$.

also promote malignant transformation. The degree of E-cadherin engagement directs the spatial arrangement of cell–matrix traction forces (Mertz *et al.*, 2013), and force transmission through E-cadherin adhesions requires coordinated modulation of local cell–ECM adhesion (Ng *et al.*, 2014). During branching morphogenesis of the salivary gland, fibrillar fibronectin can increase cell–matrix adhesion concomitantly with a loss of cell–cell adhesion to promote the formation of epithelial clefts (Sakai *et al.*, 2003). Furthermore, planar cell polarity signaling regulates the spatiotemporal assembly of fibronectin by transfering tension from cadherin-based adhesions to integrins (Dzamba *et al.*, 2009). In colon cancer cells, integrin signaling is required for Src-induced internalization of E-cadherin (Avizienyte *et al.*, 2002). In ovarian carcinoma cells, integrin clustering induces MMP-dependent shedding of the E-cadherin ectodomain, which allows cells to migrate independently (Symowicz *et al.*, 2007). Here we found that ILK modulates the balance between adherens junctions and focal adhesions in mammary epithelial cells, which regulates cell shape and acts as an essential component in cell-fate decisions downstream of TGFβ1. Of note, depleting ILK not only results in decreased levels of phosphorylated FAK but also abolishes the ability of stiff matrices to induce the phosphorylation of this focal adhesion protein. These results suggest that ILK may be required for stiffness-dependent assembly and activation of focal adhesions. Examining how ILK mediates the cross-talk between cell–cell and cell–ECM adhesions may contribute to a more comprehensive understanding of the cellular adhesive network. Future work should also focus on elucidating how signaling inputs from cell–cell and cell–ECM adhesion are integrated to trigger the switch between EMT and apoptosis.

MATERIALS AND METHODS

Request a protocol through *Bio-protocol*.

Cell culture and reagents

NMuMG mouse mammary epithelial cells (passed at a 1:10 ratio and used before passage 20) were obtained from the American Type Culture Collection and cultured in high glucose DMEM (HyClone) supplemented with 10% fetal bovine serum (Atlanta Biologicals) and 50 μg/ml gentamicin (Life Technologies); cells were confirmed to be free of mycoplasma using a commercially available kit (Lonza). NMuMG cells were seeded at a density of 50,000 cells/cm^2 on plastic or fibronectin-coated polyacrylamide substrata of soft (*E*~130 Pa) or stiff (*E*~4020 Pa) compliances and cultured at 37°C and 5% CO_2 as described previously (Lee *et al.*, 2012). Cells were cultured for 8–10 h before treatment with TGFβ1 (2 ng/ml; Peprotech) and/or FAK inhibitor (PF-573228; Sigma), which were added to the culture medium. Cells were subsequently cultured for 6 and 12 h (immunofluorescence), 24 h (caspase-3 activity, immunoblotting, immunofluorescence), or 48 h (immunofluorescence).

To knock down the expression of ILK, NMuMG cells were transduced with lentiviral particles carrying two shRNAs against ILK (sc-35667-V and sc-35666-V; Santa Cruz) or control lentivirus expressing a scrambled shRNA sequence. Stable shRNA-expressing

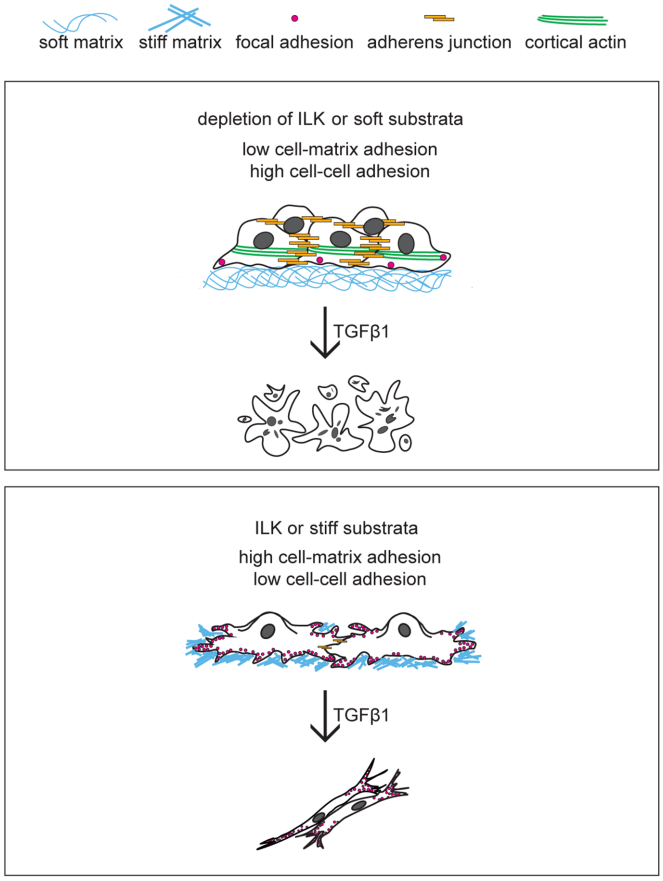

FIGURE 8: ILK controls cell fate downstream of TGFβ1 by modulating the balance between cell–cell and cell–matrix adhesion. Similar to soft matrix, depletion of ILK increases cell–cell adhesion and decreases cell–matrix adhesion, promoting apoptosis downstream of TGFβ1. In contrast, a stiff microenvironment leads to elevated cell–matrix adhesion and promotes EMT downstream of TGFβ1.

clones were produced according to the manufacturer's instructions and selected using puromycin.

Micropatterned substrata

Single-cell-sized islands (30 × 30 μm^2) of fibronectin were prepared as described previously (Gomez *et al.*, 2010). Briefly, sterile stamps of polydimethylsiloxane (PDMS; Sylgard 184) were coated with 25 μg/ml fibronectin (BD Biosciences, Franklin Lakes, NJ) in phosphate-buffered saline (PBS) overnight at 4°C and dried under compressed nitrogen. Fibronectin was microcontact-printed onto custom-made, UV/ozone-treated, PDMS-coated glass-bottom tissue culture dishes, and unstamped regions were blocked with 1% Synperonic F108 (Fluka, Buchs, Germany) in PBS. Cells were then seeded at a density of 50,000 cells per sample and allowed to adhere to the resulting islands of fibronectin.

Time-lapse imaging

Time-lapse movies were acquired using a Hamamatsu C4742-95 camera attached to a Nikon Ti-U inverted microscope and fitted with an environmental chamber held at 90% humidity, 37°C, and 5% CO_2 (Pathology Devices, Westminster, MD). Images were acquired at 10× magnification every 30 min for a total of 48 h.

Immunofluorescence analysis

Samples were fixed with 4% paraformaldehyde for 15 min, washed with PBS, and then permeabilized with 0.3% Triton X-100 for 30 min. After blocking for 1 h with 5% goat serum (Sigma) and 2% bovine serum albumin, the samples were incubated with primary antibody against E-cadherin (3195, 1:300; Cell Signaling), Snail (3895, 1:300; Cell Signaling), αSMA (A5228, 1:200; Sigma), ZO1 (40-2200, 1:300; Thermo Fisher Scientific), vimentin (V2258, 1:200; Sigma), cleaved caspase-3 (9961, 1:200; Cell Signaling), FAK (ab40794, 1:200; Abcam), pY397-FAK (44-625G, 1:50; Invitrogen), paxillin (ab32084, 1:200; Abcam), pY118-paxillin (44-722G, 1:200; Invitrogen), α-catenin (ab51032, 1:200; Abcam), or β-catenin (D10A8, 1:100; Cell Signaling). Samples were then washed with PBS and incubated with Alexa Fluor–conjugated secondary antibodies (1:200; Invitrogen). Nuclei were counterstained with Hoechst 33342 (1:1000; Invitrogen). After additional washes with PBS, samples were visualized using a 20×/0.45 NA air objective on a Nikon Eclipse Ti-U inverted fluorescence microscope (Nikon) equipped with a Hamamatsu ORCA charge-coupled device camera. Image analysis was performed on at least 200 cells for each experimental group over three independent experiments using ImageJ.

Caspase-3 activity assay

Caspase-3 activity was determined using an EnzChek Caspase-3 Assay Kit #2 (Invitrogen) according to the manufacturer's instructions. Caspase-3 activity was normalized to the total cell number as determined using a hemacytometer.

Soluble and insoluble protein fractionation assay

To separate insoluble (membrane-bound) and soluble (intracellular) fractions of adherens junction proteins, cells were lysed in cytoskeletal buffer (300 mM sucrose, 10 mM PIPES, pH 6.8, 50 mM NaCl, 3 mM MgCl2, 0.5% Triton X-100) containing complete protease inhibitors (Roche). The lysates were incubated on ice for 15 min, passed through a 27-gauge needle four times, and then centrifuged at 14,000 rpm for 20 min at 4°C. The supernatant was collected as the soluble fraction. The pellet was solubilized in 8% SDS lysis buffer, followed by sonication and centrifuged at 14,000 rpm for 10 min and collected as the insoluble fraction. Protein concentrations were measured in each sample, followed by immunoblotting analysis.

Immunoblotting analysis

Samples were lysed in RIPA lysis buffer (Thermo Scientific) supplemented with Complete protease inhibitor cocktail (Roche) and protein concentrations were measured using the detergent-compatible Protein Assay Kit (Bio-Rad). Samples were then mixed with Laemmli sample buffer, boiled at 95°C for 5 min, resolved by SDS–PAGE, and transferred to nitrocellulose membranes. Membranes were then blocked in 5% nonfat milk in 0.1% Tween-20 in Tris-buffered saline and incubated overnight at 4°C in blocking buffer containing antibodies specific for ILK (3862, 1:1000; Cell Signaling), E-cadherin (3195, 1:1000; Cell Signaling), vimentin (V5255, 1:1000; Cell Signaling), Snail (3895, 1:500; Cell Signaling), αSMA (A5228, 1:500; Sigma), FAK (3285S, 1:500; Cell Signaling), pY397-FAK (44625G, 1:500; Invitrogen), paxillin (ab32084, 1:1000; Abcam), pY118-paxillin (44722G, 1:1000; Invitrogen), α-catenin (ab51032, 1:3500; Abcam), β-catenin (ab32572, 1:3500; Abcam), or GAPDH (3683S, 1:1000; Cell Signaling). Bands were detected using horseradish-peroxidase–conjugated secondary antibodies (1:5000; Cell Signaling) and Amersham ECL Western Blotting Reagent (GE Healthcare) as a chemiluminescent substrate. Densitometry analysis was performed using ImageJ.

Scratch wound assay

Confluent monolayers of shcntl or shILK cells were treated with TGFβ1 (2 ng/ml; Peprotech) for 24 h. Monolayers were then scratched with pipette tips and washed once with culture medium to remove cellular debris. Time-lapse images were acquired at 10× magnification every 30 min for a total of 40 h. Wound areas were calculated using the ImageJ Wound Healing Tool plugin (Volker Baeker) for at least three independent experiments.

Cell tracking analysis

Cell tracking analysis was conducted on ImageJ software using the Manual Tracking plugin (Fabrice Cordeli). For each of 20 tracks per condition, one cell was manually followed through a series of half-hour or 1-h interval stacks. Once the cell remained relatively stationary in the frame, the track was completed. Cell speed data were collected from the output of the plugin for analysis.

Statistical analysis

Data represent the results of at least three independent experiments; sample number and sizes are reported in the figure legends. All statistical analyses were performed using GraphPad Prism 5.0, following the recommendations in the Prism statistics guide. Statistical comparisons of means for normally distributed data were conducted using an unpaired Student's *t* test (equal variances; Figure 6B; Supplemental Figure S5), paired *t* test (Gaussian distribution; Figure 6D), Welch's *t* test (unequal variances; Supplemental Figure S2), one-way ANOVA with Tukey–Kramer multiple comparisons test (Supplemental Figure S4), or two-way ANOVA with Tukey multiple comparisons test (Figures 1D and 7B). Normality was determined using either the D'Agostino–Pearson test (for large samples) or the Shapiro–Wilk test (for all others). $P < 0.05$ was considered to represent a significant difference between experimental groups.

ACKNOWLEDGMENTS

This work was supported in part by grants from the National Institutes of Health (CA187692, CA214292), the David & Lucile Packard Foundation, the Camille & Henry Dreyfus Foundation, and a Faculty

Scholars Award from the Howard Hughes Medical Institute. A.N.K. was supported in part by a postdoctoral fellowship from the New Jersey Commission on Cancer Research.

REFERENCES

Avizienyte E, Wyke AW, Jones RJ, McLean GW, Westhoff MA, Brunton VG, Frame MC (2002). Src-induced de-regulation of E-cadherin in colon cancer cells requires integrin signalling. Nat Cell Biol 4, 632–638.

Bachir AI, Horwitz AR, Nelson WJ, Bianchini JM (2017). Actin-based adhesion modules mediate cell interactions with the extracellular matrix and neighboring cells. Cold Spring Harb Perspect Biol 9, a023234.

Behrens J, Mareel MM, Van Roy FM, Birchmeier W (1989). Dissecting tumor cell invasion: epithelial cells acquire invasive properties after the loss of uvomorulin-mediated cell-cell adhesion. J Cell Biol 108, 2435–2447.

Cicchini C, Laudadio I, Citarella F, Corazzari M, Steindler C, Conigliaro A, Fantoni A, Amicone L, Tripodi M (2008). TGFbeta-induced EMT requires focal adhesion kinase (FAK) signaling. Exp Cell Res 314, 143–152.

Cichon MA, Nelson CM, Radisky DC (2015). Regulation of epithelial-mesenchymal transition in breast cancer cells by cell contact and adhesion. Cancer Inform 14, 1–13.

Dzamba BJ, Jakab KR, Marsden M, Schwartz MA, DeSimone DW (2009). Cadherin adhesion, tissue tension, and noncanonical Wnt signaling regulate fibronectin matrix organization. Dev Cell 16, 421–432.

Elad N, Volberg T, Patla I, Hirschfeld-Warneken V, Grashoff C, Spatz JP, Fassler R, Geiger B, Medalia O (2013). The role of integrin-linked kinase in the molecular architecture of focal adhesions. J Cell Sci 126, 4099–4107.

Franco DL, Mainez J, Vega S, Sancho P, Murillo MM, de Frutos CA, Del Castillo G, Lopez-Blau C, Fabregat I, Nieto MA (2010). Snail1 suppresses TGF-beta-induced apoptosis and is sufficient to trigger EMT in hepatocytes. J Cell Sci 123, 3467–3477.

Friedl P, Alexander S (2011). Cancer invasion and the microenvironment: plasticity and reciprocity. Cell 147, 992–1009.

Gal A, Sjoblom T, Fedorova L, Imreh S, Beug H, Moustakas A (2008). Sustained TGF beta exposure suppresses Smad and non-Smad signalling in mammary epithelial cells, leading to EMT and inhibition of growth arrest and apoptosis. Oncogene 27, 1218–1230.

Gomez EW, Chen QK, Gjorevski N, Nelson CM (2010). Tissue geometry patterns epithelial-mesenchymal transition via intercellular mechanotransduction. J Cell Biochem 110, 44–51.

Guasch G, Schober M, Pasolli HA, Conn EB, Polak L, Fuchs E (2007). Loss of TGFbeta signaling destabilizes homeostasis and promotes squamous cell carcinomas in stratified epithelia. Cancer Cell 12, 313–327.

Han S, Pang MF, Nelson CM (2018). Substratum stiffness tunes proliferation downstream of Wnt3a in part by regulating integrin-linked kinase and frizzled-1. J Cell Sci 131.

Heldin CH, Vanlandewijck M, Moustakas A (2012). Regulation of EMT by TGFbeta in cancer. FEBS Lett 586, 1959–1970.

Iordanskaia T, Nawshad A (2011). Mechanisms of transforming growth factor beta induced cell cycle arrest in palate development. J Cell Physiol 226, 1415–1424.

Lee J, Choi JH, Joo CK (2013). TGF-beta1 regulates cell fate during epithelial-mesenchymal transition by upregulating survivin. Cell Death Dis 4, e714.

Lee K, Chen QK, Lui C, Cichon MA, Radisky DC, Nelson CM (2012). Matrix compliance regulates Rac1b localization, NADPH oxidase assembly, and epithelial-mesenchymal transition. Mol Biol Cell 23, 4097–4108.

Lehembre F, Yilmaz M, Wicki A, Schomber T, Strittmatter K, Ziegler D, Kren A, Went P, Derksen PW, Berns A, *et al.* (2008). NCAM-induced focal adhesion assembly: a functional switch upon loss of E-cadherin. EMBO J 27, 2603–2615.

Leight JL, Wozniak MA, Chen S, Lynch ML, Chen CS (2012). Matrix rigidity regulates a switch between TGF-beta1-induced apoptosis and epithelial-mesenchymal transition. Mol Biol Cell 23, 781–791.

Li Y, Yang J, Dai C, Wu C, Liu Y (2003). Role for integrin-linked kinase in mediating tubular epithelial to mesenchymal transition and renal interstitial fibrogenesis. J Clin. Invest 112, 503–516.

Mege RM, Ishiyama N (2017). Integration of cadherin adhesion and cytoskeleton at adherens junctions. Cold Spring Harb Perspect Biol 9.

Mertz AF, Che Y, Banerjee S, Goldstein JM, Rosowski KA, Revilla SF, Niessen CM, Marchetti MC, Dufresne ER, Horsley V (2013). Cadherin-based intercellular adhesions organize epithelial cell-matrix traction forces. Proc Natl Acad Sci USA 110, 842–847.

Mui KL, Chen CS, Assoian RK (2016). The mechanical regulation of integrin-cadherin crosstalk organizes cells, signaling and forces. J Cell Sci 129, 1093–1100.

Ng MR, Besser A, Brugge JS, Danuser G (2014). Mapping the dynamics of force transduction at cell-cell junctions of epithelial clusters. eLife 3, e03282.

Paszek MJ, Zahir N, Johnson KR, Lakins JN, Rozenberg GI, Gefen A, Reinhart-King CA, Margulies SS, Dembo M, Boettiger D, *et al.* (2005). Tensional homeostasis and the malignant phenotype. Cancer Cell 8, 241–254.

Qin Y, Capaldo C, Gumbiner BM, Macara IG (2005). The mammalian Scribble polarity protein regulates epithelial cell adhesion and migration through E-cadherin. J Cell Biol 171, 1061–1071.

Ratheesh A, Yap AS (2012). A bigger picture: classical cadherins and the dynamic actin cytoskeleton. Nat Rev Mol Cell Biol 13, 673–679.

Rice AJ, Cortes E, Lachowski D, Cheung BCH, Karim SA, Morton JP, Del Rio Hernandez A (2017). Matrix stiffness induces epithelial-mesenchymal transition and promotes chemoresistance in pancreatic cancer cells. Oncogenesis 6, e352–e352.

Sakai T, Larsen M, Yamada KM (2003). Fibronectin requirement in branching morphogenesis. Nature 423, 876–881.

Serrano I, McDonald PC, Lock FE, Dedhar S (2013). Role of the integrin-linked kinase (ILK)/Rictor complex in TGFbeta-1-induced epithelial-mesenchymal transition (EMT). Oncogene 32, 50–60.

Somasiri A, Howarth A, Goswami D, Dedhar S, Roskelley CD (2001). Overexpression of the integrin-linked kinase mesenchymally transforms mammary epithelial cells. J Cell Sci 114, 1125–1136.

Symowicz J, Adley BP, Gleason KJ, Johnson JJ, Ghosh S, Fishman DA, Hudson LG, Stack MS (2007). Engagement of collagen-binding integrins promotes matrix metalloproteinase-9-dependent E-cadherin ectodomain shedding in ovarian carcinoma cells. Cancer Res 67, 2030–2039.

Varga J, Greten FR (2017). Cell plasticity in epithelial homeostasis and tumorigenesis. Nat Cell Biol 19, 1133–1141.

Weber GF, Bjerke MA, DeSimone DW (2011). Integrins and cadherins join forces to form adhesive networks. J Cell Sci 124, 1183–1193.

Wei SC, Fattet L, Tsai JH, Guo Y, Pai VH, Majeski HE, Chen AC, Sah RL, Taylor SS, Engler AJ, Yang J (2015). Matrix stiffness drives epithelial-mesenchymal transition and tumour metastasis through a TWIST1-G3BP2 mechanotransduction pathway. Nat Cell Biol 17, 678–688.

Yang Y, Pan X, Lei W, Wang J, Song J (2006). Transforming growth factor-beta1 induces epithelial-to-mesenchymal transition and apoptosis via a cell cycle-dependent mechanism. Oncogene 25, 7235–7244.